



This is a repository copy of *Synthesis of pH-responsive tertiary amine methacrylate polymer brushes and their response to acidic vapour*.

White Rose Research Online URL for this paper:
<http://eprints.whiterose.ac.uk/78387/>

Article:

Fielding, L.A., Edmondson, S. and Armes, S.P. (2011) Synthesis of pH-responsive tertiary amine methacrylate polymer brushes and their response to acidic vapour. *Journal of Materials Chemistry*, 21 (32). 11773 - 11780. ISSN 0959-9428

<https://doi.org/10.1039/c1jm11412c>

Reuse

Unless indicated otherwise, fulltext items are protected by copyright with all rights reserved. The copyright exception in section 29 of the Copyright, Designs and Patents Act 1988 allows the making of a single copy solely for the purpose of non-commercial research or private study within the limits of fair dealing. The publisher or other rights-holder may allow further reproduction and re-use of this version - refer to the White Rose Research Online record for this item. Where records identify the publisher as the copyright holder, users can verify any specific terms of use on the publisher's website.

Takedown

If you consider content in White Rose Research Online to be in breach of UK law, please notify us by emailing eprints@whiterose.ac.uk including the URL of the record and the reason for the withdrawal request.



eprints@whiterose.ac.uk
<https://eprints.whiterose.ac.uk/>

promoting access to White Rose research papers



Universities of Leeds, Sheffield and York
<http://eprints.whiterose.ac.uk/>

This is an author produced version of a paper published in **Journal of Materials Chemistry**.

White Rose Research Online URL for this paper:

<http://eprints.whiterose.ac.uk/78387>

Published paper

Fielding, L.A., Edmondson, S. and Armes, S.P. (2011) *Synthesis of pH-responsive tertiary amine methacrylate polymer brushes and their response to acidic vapour*. *Journal of Materials Chemistry*, 21 (32). 11773 - 11780. ISSN 0959-9428

<http://dx.doi.org/10.1039/c1jm11412c>

White Rose Research Online
eprints@whiterose.ac.uk

Synthesis of pH-responsive tertiary amine methacrylate polymer brushes and their response to acidic vapour

Lee A. Fielding¹, Steve Edmondson^{2*} and Steven P. Armes¹

¹ Dainton Building, Department of Chemistry, The University of Sheffield, Brook Hill, Sheffield, S3 7HF, UK.

² Department of Materials, Loughborough University, Loughborough, LE11 3TU, UK

ABSTRACT. Weak polyelectrolyte brushes exhibit pH-responsive swelling behaviour, tuneable surface energy, and some promise as “smart” responsive coatings. In this paper, we demonstrate the growth of two weak polybase brushes by surface-initiated atom transfer radical polymerisation (SI-ATRP) using electrostatically adsorbed polyelectrolyte macro-initiators. Poly[2-(diethylamino)ethyl methacrylate] (PDEA) and poly[2-(diisopropylamino)ethyl methacrylate] (PDPA) brushes of 150 and 170 nm thickness respectively were grown within 22 h at 20 °C. Using *in situ* ellipsometry an acid-induced swelling transition was observed at pH 7.4 for PDEA and pH 6.5 for PDPA, similar to the pK_a values reported for the corresponding free polymer chains. The kinetics of brush swelling involves an initially fast regime followed by a subsequent slower regime. Reversible surface energy switching with pH modulation was also demonstrated by contact angle goniometry. Finally, it was demonstrated that PDPA brushes respond to the presence of acidic vapours. On exposure to humid HCl vapour, such brushes become hydrophilic, resulting in water uptake and swelling, producing a visible change in the thin film interference colour.

Introduction

Surface-initiated polymerisation (SIP) is the growth of polymer chains from initiators immobilised on a substrate.¹ Polymers produced in this way often have a chain grafting density which is sufficiently high to ensure that the polymer chains are in the *polymer brush* regime.² Typically, controlled radical polymerisation is used for the polymer growth to provide good control over the brush layer thickness, polydispersity and also to allow the synthesis of block copolymers.³ Brushes of responsive polymers grown by SIP are increasingly widely studied.⁴ Surface grafting produces brush layers with excellent stability towards degrafting, which is desirable when studying polymers in a good solvent (such as polyelectrolytes in water). The high grafting density produced by SIP gives thick films (with reported dry thicknesses of up to 600 nm by controlled radical polymerisation⁵ and up to 5 µm by ring-opening metathesis polymerisation⁶), which allows changes in brush thickness to be monitored by ellipsometry and AFM, both in the dry state and when immersed in solvent.^{7,8}

Polyelectrolyte brushes have attracted much theoretical and practical interest.^{9,10} SIP has been used to grow polyelectrolyte brushes in the majority of recent studies, with the literature including many examples of both strong polyelectrolytes (*quenched*, i.e. charged under all conditions) and weak polyelectrolytes (*annealed*, with a dissociation constant that depends on pH and ionic strength).

For weak polyelectrolyte brushes, the transition with pH from uncharged to charged grafted chains causes increased inter-chain repulsion (coulombic repulsion) and increased osmotic pressure due to counter-ions, which can produce large changes in layer thickness.^{9,10} If the build-up of charge density is also accompanied by a switch in solubility, from a fully collapsed hydrophobic brush to a hydrophilic brush, the change in film

thickness observed in water is usually substantial. Weak polyelectrolyte brushes have been utilised for the fabrication of pH-selective membranes,¹¹ pH-controlled actuators,¹² pH-triggered controlled release,¹³ pH-sensitive “chemical gates” for microfluidics,¹⁴ and as a component in a switchable adhesive bond.¹⁵

There have been a number of reported examples of weak cationic polyelectrolyte brushes of poly(2-(dimethylamino)ethyl methacrylate) (PDMA) grown by SIP (see for example Ding et al.¹⁶ and references therein). Although PDMA brushes show increased swelling on protonation at pHs below the pK_a^{17,18} they are water-soluble in both their protonated and deprotonated states.

In this work, we grow brushes from two tertiary amine methacrylates closely related to DMA: 2-(diethylamino)ethyl methacrylate (DEA) and 2-(diisopropylamino)ethyl methacrylate (DPA). Whereas PDMA and PDEA have similar pK_a values (7.0 and 7.3 respectively, as measured for untethered homopolymers in dilute solution), PDPA has a significantly lower pK_a (6.3).¹⁹ In addition, while PDMA is water-soluble in both its protonated and unprotonated state, the more hydrophobic PDEA and PDPA chains show pH-dependent solubility, being solvated only when protonated (i.e. below their pK_a values).²⁰

In contrast to the well-studied PDMA brushes, PDEA brushes have received rather less attention,^{13,16,21–26} while there appear to be only two previous studies of PDPA brushes.^{22,27} Therefore, we begin by demonstrating the growth of PDEA and PDPA brushes by surface-initiated ATRP, investigating the effect of both the initiator density and the nature of the copper catalyst used for SIP.

We then study the pH-induced swelling of these brushes using *in situ* ellipsometry to attempt to reproduce a prior report that the pK_a of PDEA brushes is significantly lower than that for untethered polymer.²³ After using contact angle goniometry to demonstrate that the surface energy of PDEA and PDPA is pH-

sensitive, we study the swelling response of brushes to acidic vapour. We anticipated that exposing dry PDPA brushes to moist acidic vapour would cause a switch to the protonated hydrophilic state, leading to water uptake and swelling. By growing brushes of a sufficient thickness that thin film interference colours are visible (typically greater than 50 nm for organic polymers on silicon wafers), such swelling should translate to a colour change. Although polymer brushes have been shown to respond to water vapour²⁸ or the presence of organic solvent vapours,^{29,30} to our knowledge this work represents the first study of the selective response to acidic vapours.

Experimental

Materials. 2-(Diisopropylamino)ethyl methacrylate (DPA) was obtained from Scientific Polymer Products, USA and passed through an “inhibitor removing column DHR-4” supplied with the monomer, glycerol monomethacrylate (GMA) (containing 8 mol % 1,3-dihydroxyisopropyl methacrylate isomeric impurity) was kindly donated by Cognis Performance Chemicals, Hythe, UK. All other reagents were obtained from either Sigma-Aldrich (Gillingham, UK) or Fisher Scientific (Loughborough, UK) and were used as received. Silicon wafers (<100> orientation, boron-doped, 0–100 Ω .cm) were purchased from Compant Technology (Peterborough, UK). Deionised water was obtained using an Elga Elgastat Option 3 system. Buffer solutions were prepared using 0.01 M solutions of borax and boric acid (“borate buffer”), monosodium phosphate and disodium phosphate (“phosphate buffer”), trisodium citrate and citric acid (“citrate buffer”).

Synthesis of polyelectrolyte macro-initiators. The synthesis of the anionic polyelectrolytic macro-initiator used in this work has been described in detail elsewhere^{22,31} and is therefore only briefly discussed here. A poly(glycerol monomethacrylate) (PGMA) precursor was synthesised using ATRP with a target degree of polymerisation of 50. In a two-step, one-pot reaction, 36 mol % of the PGMA hydroxy groups were esterified with BIBB before 72% of the remaining hydroxyl groups were esterified with excess 2-sulfobenzoic acid cyclic anhydride, giving a total degree of esterification of 82% (i.e. 18 mol % unreacted hydroxyl groups). GPC analysis of the PGMA precursor indicated an M_n of 12,400 and a M_w/M_n of 1.31 against poly(methyl methacrylate) standards. The cationic macro-initiator used here is also similar to that reported previously,^{31,32} with monohydroxyl-functional 2-hydroxyethyl methacrylate (HEMA) replaced by dihydroxy-functional glycerol monomethacrylate (GMA) in order to increase the initiator density. Briefly, this macro-initiator was prepared by statistical copolymerisation of glycerol monomethacrylate (GMA) with 2-(dimethylamino)ethyl methacrylate (DMA) using ATRP. The statistical copolymer precursor comprised 50 mol % DMA and 50 mol % GMA and its target degree of polymerisation was 80. ¹H NMR spectroscopy confirmed complete esterification of the hydroxyl groups using 2-bromoisobutyryl bromide (BIBB) and complete quaternisation of the tertiary amine groups using methyl iodide. GPC analysis of the copolymer precursor indicated an M_n of 21,200 and a M_w/M_n of 1.34 against poly(methyl methacrylate) standards.

Macroinitiator adsorption. Silicon wafers were cleaned and rendered hydrophilic by first washing with acetone, propan-2-ol and water, and then immersed for 15 min. in a mixture of

ammonia solution (28 mL, 35% wt), hydrogen peroxide solution (28 mL, 30% wt) and water (142 mL) at 75 °C. Wafers were removed, rinsed thoroughly with water and dried under a stream of nitrogen. For anionic macro-initiator adsorption, wafers were then amine-functionalised by exposure to (3-aminopropyl)triethoxysilane (APTES) vapour at 0.2 mbar for 30 min. at room temperature and then annealed in air for 30 min. at 110 °C. Wafers were then immersed in 1 g L⁻¹ aqueous solutions of cationic and anionic macro-initiator overnight followed by thorough rinsing with water.

Surface-initiated ATRP of DPA (typical protocol). DPA, propan-2-ol and water were separately degassed by nitrogen purging for 30 min. DPA (10 g, 46.9 mmol), propan-2-ol (9.5 ml), and water (0.5 ml) were transferred by syringe into a flask, followed by Cu(I)Br (112 mg, 0.8 mmol), and 2,2'-bipyridine (268 mg, 1.8 mmol); this mixture was stirred under a nitrogen purge to aid dissolution. Aliquots were transferred by syringe to Schlenk tubes (contained in a “Carousel 12 Reaction Station”, Radleys, UK) containing ca. 1 cm² pieces of macroinitiator-coated wafer under nitrogen. After various times, individual tubes were opened to the air and the PDPA brush-coated wafers were removed. To remove the ATRP catalyst and monomer, each wafer was rinsed thoroughly with propan-2-ol, water and methanol followed by drying under a stream of nitrogen.

Surface-initiated ATRP of DEA (typical protocol). DEA, methanol and water were separately degassed by nitrogen purging for 30 min. DEA (10 g, 54.0 mmol), methanol (8.0 ml), and water (2.0 ml) were transferred by syringe into a flask, followed by Cu(I)Br (129 mg, 0.9 mmol), Cu(II)Br₂ (60 mg, 0.3 mmol) and 2,2'-bipyridine (393 mg, 2.5 mmol); this mixture was stirred under a nitrogen purge to aid dissolution. Aliquots were transferred by syringe to Schlenk tubes (contained in a “Carousel 12 Reaction Station”, Radleys, UK) containing ca. 1 cm² pieces of macro-initiator-coated wafer under nitrogen. After various times, individual tubes were opened to the air and the PDEA brush-coated wafers were removed. To remove the ATRP catalyst and monomer, each wafer was rinsed thoroughly with water and methanol followed by drying under a stream of nitrogen.

Characterisation. All ellipsometric studies were conducted using a phase-modulated spectroscopic ellipsometer (Uvisel, Jobin Yvon) with an angle of incidence of 70°. Measurements were conducted from 300 to 700 nm and modelling was performed using WVASE software (J. A. Woolam Co., USA). Fit quality was assessed using the root mean square error (RMSE) between the measured and modelled ellipsometric constants Δ and Ψ over all measured wavelengths. The dry films were modelled as a single layer of variable thickness with refractive index given by the Cauchy parameters of $A_n = 1.4615$, $B_n = 0.00514 \mu\text{m}^2$ (found by fitting these values for a thick PDPA film). *In situ* aqueous ellipsometry was conducted in the presence of 0.01 M buffer solutions (citrate for pH < 6.6, phosphate for pH 5.6–8.2 and borate for pH > 7.3) across a range of pH values inside a home-made liquid cell. To ensure that the desired pH was obtained, the sample cell was rinsed several times with deionised water in between each buffer solution. The ellipsometric parameters of the films were monitored continuously at 500 nm to ensure equilibrium had been reached before carrying out the

spectroscopic scan. *In situ* ellipsometric data were modelled as a single slab with a refractive index given by a linear effective medium approximation (EMA) between polymer and water. The model was fitted using two adjustable parameters: the slab thickness and the polymer volume fraction in the EMA. Studies of the response of polymer films to various atmospheres were also conducted using ellipsometry. In this case, compressed air impinged on the sample after passage through either a silica gel drying column ("dry air"), a water bubbler ("wet air"), or concentrated HCl ("wet acidic air"). Modelling was carried out by fitting both the ellipsometric thickness and the Cauchy parameter A_n .

Advancing contact angle measurements were obtained using drops of the appropriate buffer solution and a syringe pump to increase the drop volume at a steady rate. Images were captured using a FujiFilm FinePix E500 digital camera and the contact angle measured using ImageJ software running the DropSnake add-on.³³ The wafers were soaked in the appropriate buffer solution for one hour between measurements to ensure equilibration.

Optical microscope images of polymer-coated samples were recorded using a James Smith (England) light microscope fitted with a Nikon Coolpix 4500 digital camera.

Simulated thin film interference colours were calculated using a simplified version of a model based on a standard thin-film matrix approach presented by Henrie et al.³⁴ The surface was modelled as a silicon substrate with a polymer overlayer, with wavelength-dependent refractive indices for both layers being the same as those used for ellipsometry. For a given polymer film thickness, the surface reflectance was calculated for incident light perpendicular to the surface at three wavelengths (610 nm, 550 nm and 470 nm, corresponding to red, green and blue respectively), using the equations given in the Supporting Information. These reflectances are converted directly to an RGB colour value in an image file by assuming equal illumination intensity at all wavelengths. Despite the simplifications used in our model compared to that of Henrie et al.³⁴ (e.g. neglecting the wavelength response function of the eye or CCD sensor used to record the image, assuming a uniform output spectrum of the illumination source, directly converting reflectance to RGB value without regard for colour-space conversion to match the output device), we are able to produce reliable simulations of thin-film colours of brushes on silicon in almost all cases we have explored.



Scheme 1 Electrostatic adsorption of anionic macroinitiator onto cationic amine-functionalised silicon wafers from aqueous solution, followed by surface-initiated ATRP of poly[2-(diethylamino)ethyl methacrylate] or poly[2-(diisopropylamino)ethyl methacrylate]. Protonation of the grafted polymers leads to cationic brush chains.

Results and Discussion

SI-ATRP from electrostatically-adsorbed macro-initiator

The first step in surface-initiated polymerisation is the immobilisation of the initiator groups onto the substrate. In this work we apply the *polyelectrolyte macro-initiator* approach, in

which a pre-formed polymer containing both 2-bromoester initiator sites and either cationic or anionic groups, is adsorbed electrostatically onto an oppositely-charged substrate.^{22,31,32,35-37}

Two polyelectrolyte macro-initiators containing 2-bromoester initiator groups were used in this work: a cationic^{31,32} macro-initiator adsorbed onto clean silicon wafers, and an anionic^{22,36} macro-initiator adsorbed onto amine-functionalised silicon wafers. We chose to use two oppositely-charged macro-initiators to allow a wide pH range to be examined in the event of desorption problems at extreme pH. For example, silica becomes less negatively charged at low pH, which in principle might weaken the electrostatic adsorption of a cationic macro-initiator. At high pH, the primary amine groups on the APTES-coated silica can become deprotonated, which could weaken the adsorption of an anionic macro-initiator. However, no such stability problems were observed with either macro-initiator in our study, demonstrating the versatility and broad applicability of the macro-initiator approach.

Polymerisation from the 2-bromoester ATRP initiator sites gives rise to polymer brushes (Scheme 1). Following our previous work,²² DEA was polymerised in 4 : 1 v/v methanol/water using Cu(I)Br catalyst and Cu(II)Br₂ deactivator. The formulation reported by McDonald and Rannard³⁸ was adopted for the growth of PDPA brushes; this involved using 95 : 5 v/v propan-2-ol/water solvent and Cu(I)Br catalyst (with no added deactivator). The thickness of each dried brush was determined via ellipsometry under ambient conditions.

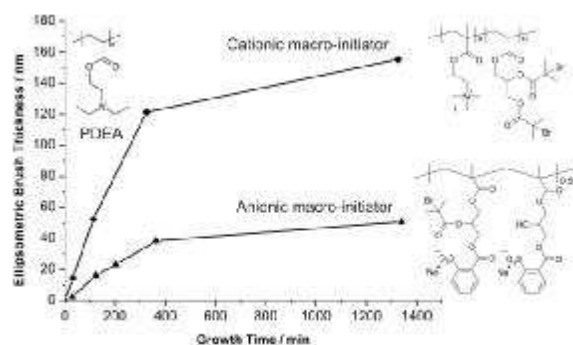


Fig. 1 Evolution of dry ellipsometric brush thickness with time for the surface-initiated polymerisation of 2-(diethylamino)ethyl methacrylate (DEA) from both anionic (▲) and cationic (◆) macro-initiators on silicon wafers. DEA was polymerised using 4 : 1 v/v methanol/water solvent mixture and a CuBr/CuBr₂ catalyst. The DEA concentration was 2.59 M and the DEA:CuBr:CuBr₂:bpy molar ratio was 60 : 1 : 0.3 : 2.8. All polymerisations were conducted at 20 °C.

Fig. 1 shows the typical evolution of ellipsometric thickness for PDEA brushes grown from adsorbed cationic and anionic macro-initiators over time. The former macro-initiator was similar to that reported by us previously.^{31,32} However, our earlier cationic macro-initiator contained a relatively low proportion of 2-bromoester initiator groups and so only produced relatively thin polymer brush films (i.e. with a low grafting density). To overcome this limitation, a new cationic macro-initiator was synthesised containing a higher proportion of 2-bromoester groups by replacing 2-hydroxyethyl methacrylate with the bifunctional glycerol monomethacrylate. This strategy was

previously successful for increasing the grafting density of brushes grown from anionic polyelectrolyte macro-initiators.²²

PDEA growth from both macro-initiators is fairly well controlled for the first 6 h at 20 °C (as characterised by the relatively constant growth rate with time expected for surface-initiated, surface-confined polymerisation), with the growth rate decreasing thereafter due to either termination or catalyst deactivation. Although the polymerisation kinetics are very similar for both macro-initiators, greater brush thicknesses were obtained for the cationic macro-initiator, presumably due to a higher grafting density.

Assuming that the two macro-initiators adsorb similarly (i.e. with the same adsorbed mass per unit area, mg m^{-2}) onto the wafers and that the grafting density is proportional to initiator density,³⁹ simple consideration of the macro-initiator structures suggests that the cationic macro-initiator should produce approximately twice the grafting density of the anionic macro-initiator. In reality, the thicknesses (and hence grafting densities) obtained with the cationic initiator are around three times greater, most likely representing some difference in the extent of deposition. Additionally, based on the observed brush layer thicknesses, our prior work with macro-initiators³⁵ and the near-linear increase in brush thickness with time achieved, it is clear that these polymer chains are in the brush regime.

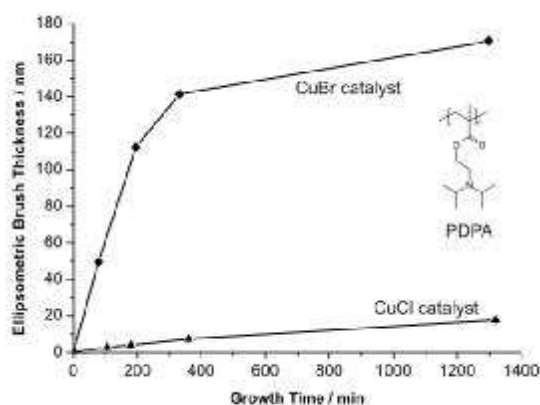


Fig. 2 Evolution of dry ellipsometric brush thickness with time for the surface-initiated polymerisation of 2-(diisopropylamino)ethyl methacrylate (DPA) from anionic macro-initiator on aminated silicon wafers. DPA was polymerised using a 95 : 5 v/v propan-2-ol/water solvent mixture and either a CuBr (◆) or a CuCl (▲) catalyst. The DPA concentration was 2.24 M, and the DPA:CuX:bpy molar ratio was 60 : 1 : 2.2, polymerisations were conducted at 20 °C. Error bars are smaller than the plotted points in all cases.

Since SI-ATRP of DPA has been hardly explored, optimisation of this brush growth was studied in some detail. As is often the case in SI-ATRP, large changes in polymerisation rate can be achieved by making modest changes to the composition of the polymerising solution. For example, it is known that using CuCl catalyst in ATRP generally results in slower polymerisations than CuBr.⁵ This effect was observed for the growth of PDPA brushes, see Fig. 2. Polymerisation of DPA catalysed by CuBr has a much greater initial growth rate than that catalysed by CuCl, with both systems exhibiting good control (linear thickness increase with

time) for the first 3 h of the polymerisation. Indeed, the polymerisation remains well controlled up to 22 h when using CuCl, whereas using CuBr leads to a retarded brush growth rate at long reaction times (most likely due to a greater radical concentration in this faster system, leading to a greater termination rate⁴⁰).

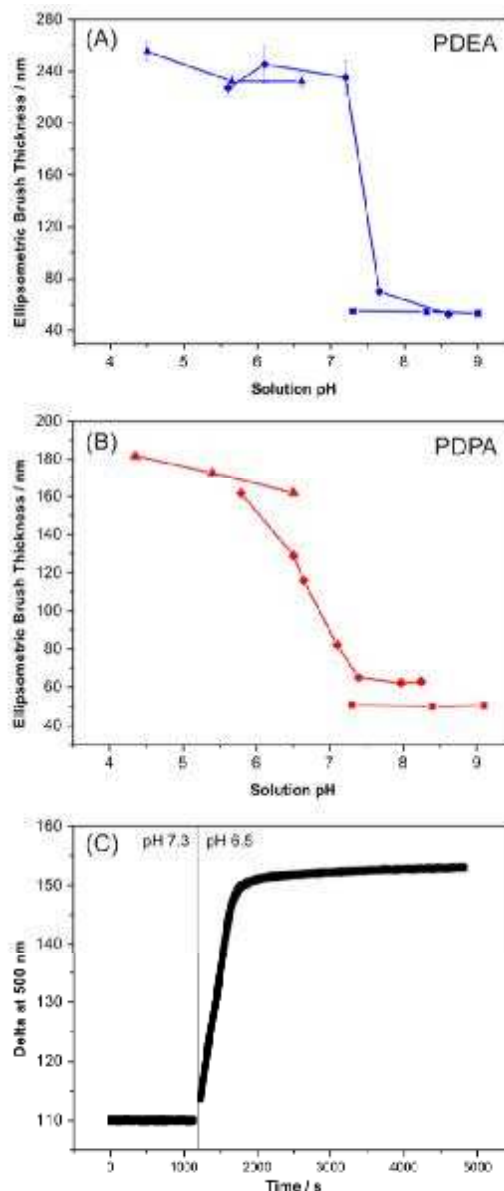


Fig. 3 (a) Aqueous *in situ* ellipsometric thickness as a function of pH for a PDEA polymer brush grown from anionic macroinitiator on aminated silicon wafers. The samples were immersed in buffer solutions (borate (■), phosphate (◆) or citrate (▲), 0.01 M) which were systematically altered from basic to acidic pH. (b) Swelling of a PDPA brush in borate, phosphate and citrate buffers (as presented in Fig. 3a). (c) Change in Δ with time for a PDPA brush upon change of buffer solution from borate to citrate. The ellipsometric parameters Δ and Ψ (not shown) were monitored to ensure that the brush swelling had reached equilibrium, followed by thickness measurements *via* a spectroscopic scan. The discontinuity in the plot is due to the temporary loss of signal whilst the solution in the cell is replaced.

pH responsive behaviour of PDPA and PDEA homopolymer brushes

Using neutron reflectometry, Geoghegan et al. have reported the onset of swelling for PDEA brushes occurs several pH units lower than the pK_a for the free polymer.²³ They propose that this effect becomes more pronounced with increasing grafting density. Indeed, the most densely grafted brush in their study is still deswollen at pH 4 (pK_a of the free polymer = 7.3¹⁹). To verify this pK_a shift for PDEA brushes, and to attempt to reproduce the effect in PDPA, brush-coated wafers (dry thicknesses = 51 nm for PDEA and 48 nm for PDPA) were exposed to buffer solutions of incrementally reduced pH and the ellipsometric parameters were recorded using *in situ* ellipsometry. After each pH change the brush was allowed to reach equilibrium, as judged by continuously monitoring the ellipsometric parameters (typical data for this equilibration are shown in Fig. 3c). Spectroscopic ellipsometric data from each equilibrated measurement were fitted using a model consisting of a single slab with a refractive index defined by a linear effective medium approximation (EMA) between pure polymer and water. Thus the model has two adjustable parameters: the slab thickness and solvent content in the EMA. The fitted slab thicknesses are presented as a function of pH for PDEA and PDPA brushes in Fig. 3a. Acceptable fits were obtained in all cases (typical RMSE < 2.0). It should be noted that the fitted polymer volume fractions were reasonably consistent with the brush swelling ratio calculated from the slab thickness (i.e. for a swelling ratio of two based on the dry brush thickness, the polymer volume fraction was approximately 0.50).

Using a phosphate buffer (which spans the range over which the swelling transition occurs), the pK_a of the brushes can be judged to be around 7.4 for PDEA and around 6.5 for PDPA, which are similar to those for the untethered polymers. Thus, we do not observe the surface pK_a shift noted by Geoghegan et al.²³

Significant differences in pK_a between brushes and free polymer for weak polyelectrolytes is not unknown, having been observed for poly(methacrylic acid) (PMAA)^{7,41} and poly(acrylic acid) (PAA)⁴¹⁻⁴⁴ with the brush pK_a being higher than the free polymer pK_a (since these are weak polyanions). It has also been shown that the magnitude of the pK_a shift is dependent on grafting density.⁴³ Therefore, it is possible that our grafting density is too low to produce a significant shift. Although dry brush thicknesses were similar, the small molecule silane initiator used by Geoghegan et al. is likely to give a higher grafting density than the macro-initiator approach used here.²²

Although a phosphate buffer spanned the pH range of interest for the swelling transition for both brushes, borate and citrate buffers were also used in this work to investigate higher and lower pH ranges respectively. It is clear that the apparent pK_a values of the brushes are different depending on the choice of buffer. For example, at pH 7.3, the PDEA brushes are fully swollen in phosphate buffer, but fully deswollen in borate buffer. Differences in ionic strength between buffers are the most likely cause of this effect.

Our buffer solutions were made up by mixing 0.01 M solutions of an acidic (less dissociated) and basic (more dissociated) form of the buffer species. Thus, with increasing pH, the ionic strength of the buffer increases considerably, although the concentration of

the buffering species remains constant. For example, tribasic phosphate (pK_a values of 2.0, 6.8 and 12.5)⁴⁵ is highly dissociated at pH 7.3 producing a relatively high ionic strength. In contrast, borate (lowest pK_a = 9.1) is mostly present as undissociated boric acid⁴⁶ at the same pH, producing a very low ionic strength.

At a pH around the pK_a of a weak polybase brush (i.e. where the brush is partially protonated), increasing the ionic strength lowers the effective pH inside the brush.⁴⁷ At very low ionic strength, the HO^- counter-ions to the charged amine groups remain confined within the brush layer to maintain electroneutrality. This confinement increases the local pH and shifts the brush protonation equilibrium towards a less charged (less swollen) state. At higher ionic strengths, buffer counter-ions (e.g. HPO_4^{2-}) can diffuse into the brush, allowing HO^- to be released into solution, and the pH within the brush layer approaches the solution pH. Thus we observe that, at pH 7.3, the PDEA brush is swollen (more protonated) in the high ionic strength phosphate buffer and deswollen (less protonated) in the low ionic strength borate buffer, leading to a shift in the apparent pK_a . Along with a possible grafting density difference, the effect of ionic strength may explain the difference between our measurements and those of Geoghegan et al.,²³ whose studies were conducted at low ionic strength (no background salt), which would be expected to lower the observed pK_a .

The same apparent pK_a shift is also observed for PDPA brushes, with greater swelling observed at pH 6.5 for the higher ionic strength citrate buffer than the phosphate buffer. The difference between the deswollen thickness of these brushes in phosphate and borate buffers (~50 nm and ~40 nm respectively) may be due to some polymer degrafting, degradation after exposure to relatively basic borate solution or varying amounts of buffer salts trapped within the deswollen brush.

At low pH, where a weak polybase brush is fully protonated, it has been shown that increasing ionic strength *reduces* brush swelling⁴⁸ due to screening of the charges by the electrolyte. In general, the degree of polyelectrolyte brush swelling is a complex non-monotonic function of ionic strength as the brush enters different swelling regimes (for example, crossing from the *osmotic brush* regime into the *salted brush* regime).^{7,44,49,50} Therefore, caution should be exercised when interpreting apparent brush pK_a values at differing ionic strength.

Typical kinetics for the brush swelling transition (on lowering the pH from 7.3 to 6.5) are shown in Fig. 3c for a PDPA brush. There is an initial rapid change in brush dimensions (over approximately 10 min), followed by a period of slower change until equilibrium is attained after more than 1 h. The initial rapid change is presumably due to the ingress of water molecules. This causes plasticisation of the polymer chains at the diffusion front, and so the more rapid entry of further water molecules.^{51,52} The slower swelling phase of the brush transition is likely to be due to relaxation processes, with the absorption of additional water molecules being made possible by conformational changes in the brush layer.²⁸ A more detailed analysis of the kinetics of swelling (presented in the Supporting Information suggests that there are in fact three discrete swelling regimes, although this may be an artefact of the simple single-slab density profile used for ellipsometric fitting. Further work is clearly warranted in this area, but this is beyond the scope of the present study.

To investigate the reversibility and magnitude of the swelling/de-swelling brush transitions, the solution pH in the liquid cell was cycled above and below that of the swelling transition by replacement with alternating phosphate buffer solutions. As above, the ellipsometric parameters were monitored to ensure equilibration, followed by a spectroscopic scan to measure the thickness. It can be seen in Fig. 4 that the brush thickness responds reversibly to this pH cycling with swelling/de-swelling occurring either side of the pK_a , as expected. Moreover, the magnitude of the swelling transition is similar for the PDEA and PDPA brushes. The fitted polymer volume fraction of the EMA was also consistent with this interpretation (i.e. low solvent content in the collapsed state, high solvent content in the swollen state).

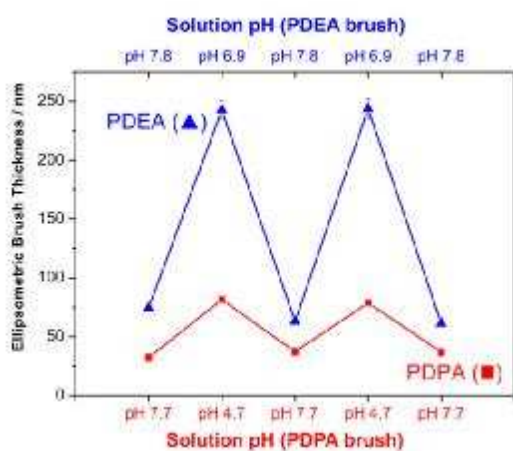


Fig. 4 Aqueous *in situ* ellipsometric thickness against pH for a PDPA (■) and a PDEA (▲) brush grown from anionic macro-initiator on aminated silicon wafers. The samples were immersed in buffer solutions with alternating pH and allowed to reach equilibrium. Dilute phosphate buffer solutions (0.01 M) were used to perform the experiment.

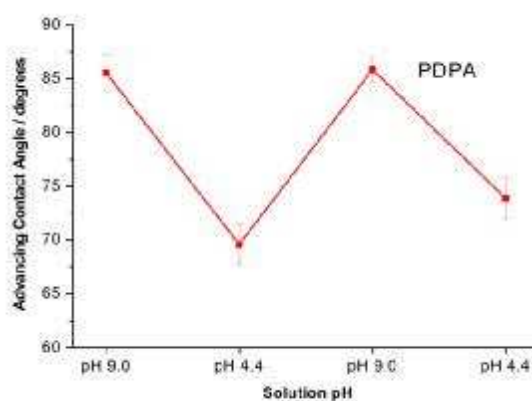


Fig. 5 Advancing contact angle against solution pH for a PDPA brush grown from anionic macro-initiator adsorbed on an aminated silicon wafer. The wafers were soaked in the appropriate 0.01 M buffer solution (citrate for pH 4.4 and borate for pH 9.0) for 1 h between measurements. Contact angles were measured using a digital camera along with ImageJ software running the DropSnake add-on.

The reversibility of the pH-response is also supported by water contact angle measurements on PDPA brushes. After soaking for 1 h in the appropriate buffer solution, the advancing water contact angle was measured using that same buffer solution (Fig. 5). This pre-treatment of the surface reduces proton transfer during drop spreading (i.e. a *non-reactive spreading protocol*⁵³), which ensures that equilibrium contact angle values are observed. As expected, these contact angle measurements reveal that the brush surface is more hydrophilic (lower contact angle) in its protonated state, and less hydrophilic (higher contact angle) in its deprotonated state. The contact angle for the protonated brush is not as low as might be expected for this water-soluble polyelectrolyte, which showed a high degree of swelling by *in situ* ellipsometry. This is most likely due to surface rearrangement of the PDPA brush chains upon drying (between soaking and contact angle measurements) to present the relatively hydrophobic isopropyl groups and/or the methacrylate backbone to the air, lowering the brush surface energy. Such surface rearrangements in response to the environment are well known⁵⁴ and should be particularly prominent in this case given that both PDEA and PDPA brushes have T_g values at around room temperature⁵⁵ allowing fast switching.

Stratakis et al. recently reported pH-switching of the PDPA contact angle, with a rather low range between protonated and deprotonated states being observed ($\sim 30^\circ$, compared with $\sim 15^\circ$ in our work).²⁷ The contact angle reported in the protonated state ($\sim 60^\circ$) was somewhat lower than that observed in our study (73°), leading to a larger contact angle 'switch'. However, Stratakis et al. measured static contact angles, which allows more time for polymer chain reorganisation to expose the cationic amine groups compared to the advancing contact angle measurements used in our work.

Acidic vapour response of PDPA homopolymer brushes

One aim of this work was to investigate the response of PDPA brushes to acidic vapours in surrounding atmosphere. A coated wafer was exposed to a sequence of different atmospheres including dry, ambient and moist air (air with varying water vapour content) and acidic conditions (moist air with HCl vapour), while the ellipsometric parameters were continuously measured. The ellipsometric thickness and the brush layer refractive index were modelled in order to determine the brush response. Fig. 6 shows that, as expected, the non-protonated brush thickness remained constant both in dry and moist conditions due to the hydrophobic nature of the neutral PDPA chains. On exposure to acidic HCl vapour, the brush thickness increased due to protonation of the amine groups and concomitant uptake of water from the moist air. After protonation, the now-hydrophilic brush is responsive towards moisture, i.e. it is de-swollen under dry conditions and the brush thickness increases with increasing water content (ambient to saturated). Once deprotonated by soaking in basic solution the PDPA brush returns to its original non-responsive state, highlighting the reversible nature of its pH-response.

A rather simpler method of following the brush swelling transition is to observe its thin film (interference) colour. Thickness-dependant colour changes of polymer brushes have been previously used to monitor the uptake of Ag^+ ions by a polyelectrolyte brush by Ramstedt et al.⁵⁶ As the brush thickness

changes, the colour of the surface can be monitored either by eye or by optical microscopy, as shown in Fig. 6 for a PDPA brush of approximately 70 nm thickness undergoing the same series of vapour treatments as the sample brush for ellipsometry studies.

The observed colour changes are consistent with those expected from our simulations of a 70 nm thick brush, with changes in brush thickness calculated using the swelling ratios derived from ellipsometry. This brush sample shows a clear colour change from brown in the unswollen state to blue in the presence of HCl vapour.

10 vapour.

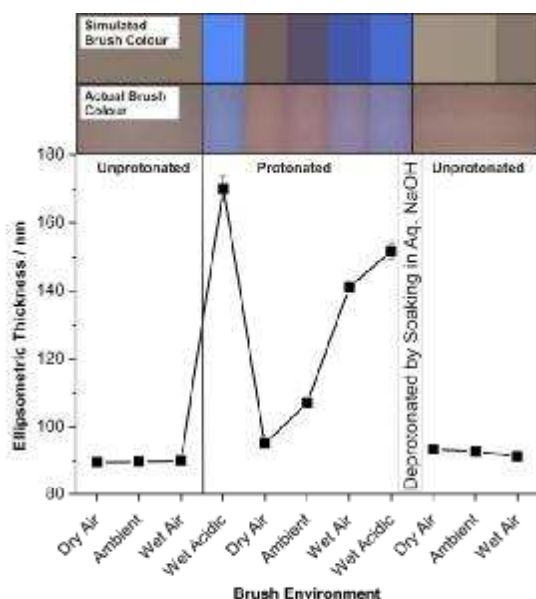


Fig. 6 Ellipsometric thickness as a function of surrounding vapour phase for a PDPA brush grown from anionic polyelectrolyte initiator adsorbed on to an aminated silicon wafer. Both Δ and Ψ parameters were monitored to ensure that equilibrium had been attained, followed by thickness measurements *via* a spectroscopic scan. To show the colorimetric response to the vapour phase, images of an approximately 70 nm thick sample undergoing the same sequence of vapour treatments were recorded using a digital camera and optical microscope. Colours were modelled as detailed in the experimental section assuming a 70 nm initial brush thickness, and swelling ratios identical to that reported by ellipsometry for the 90 nm sample.

Conclusions

We have demonstrated the growth of polymer brushes based on two tertiary amine methacrylates by surface-initiated ATRP. Both PDEA and PDPA brushes display reversible pH-dependent swelling and surface energy changes, as probed by *in situ* ellipsometry and contact angle goniometry. PDPA brushes respond to the presence of acidic vapour. In humid HCl vapour, the chains become protonated and water-swella-
 25 ble, leading to a dramatic increase in thickness. By growing brushes of an appropriate initial thickness, this acid-triggered swelling also produces a concomitant colour change. We are currently working to extend this principle to produce polymer brushes which display
 30 a swelling response in the presence of other gaseous species.

Acknowledgements

Dr Cong Duan Vo is thanked for the synthesis of the cationic macroinitiator. Dr Simon Martin, Dr Simon Titmuss and Dr Andrew Parnell are thanked for valuable discussions. DSTL is acknowledged for funding a summer studentship for L.A.F. EPSRC is acknowledged for post-doctoral platform grant GR/S25845/01 (S.E.).

References

1. S. Edmondson, V. L. Osborne and W. T. S. Huck, Chem. Soc. Rev., 2004, 33, 14
2. W. J. Brittain and S. J. Minko, J. Polym. Sci., Part A: Polym. Chem., 2007, 45, 3505
3. R.I. Barbey, L. Lavanant, D. Paripovic, N. Schüwer, C. Sugnaux, S. Tugulu and H.-A. Klok, Chem. Rev., 2009, 109, 5437–5527
4. S. Minko, Polym. Rev., 2006, 46, 397–420
5. W. Huang, J.-B. Kim, M. L. Bruening and G. L. Baker, Macromolecules, 2002, 34, 1175–1179
6. A. Juang, O. A. Scherman, R. H. Grubbs and N. S. Lewis, Langmuir, 2001, 17, 1321–1323
7. A. J. Parnell, S. J. Martin, C. C. Dang, M. Geoghegan, R. A. L. Jones, C. J. Crook, J. R. Howse and A. J. Ryan, Polymer, 2009, 50, 1005–1014
8. S. Edmondson, N. T. Nguyen, A. L. Lewis and S. P. Armes, Langmuir, 2010, 26, 7216–7226
9. M. Ballauff and O. Borisov, Curr. Opin. Colloid Interface Sci., 2006, 11, 316–323
10. J. Rühle, M. Ballauff, M. Biesalski, P. Dziezok, F. Gröhn, D. Johannsmann, N. Houbenov, N. Hugenberg, R. Konradi, S. Minko, M. Motornov, R. R. Netz, M. Schmidt, C. Seidel, M. Stamm, T. Stephan, D. Usov and H. Zhang, Advances in Polymer Science, 2004, 165, 79
11. H. Iwata, I. Hirata and Y. Ikada, Macromolecules, 1998, 31, 3671–3678
12. F. Zhou, W. Shu, M. E. Welland and W. T. S. Huck, J. Am. Chem. Soc., 2006, 128, 5326–5327
13. J. T. Sun, C. Y. Hong and C. Y. Pan, J. Phys. Chem. C, 2010, 114, 12481–12486
14. L. Ionov, N. Houbenov, A. Sidorenko, M. Stamm and S. Minko, Adv. Funct. Mater., 2006, 16, 1153–1160
15. R. La Spina, M. R. Tomlinson, L. Ruiz-Perez, A. Chiche, S. Langridge and M. Geoghegan, Angew. Chem., Int. Ed., 2007, 46, 6460–6463
16. S. J. Ding, J. A. Floyd and K. B. Walters, J. Polym. Sci., Part A: Polym. Chem., 2009, 47, 6552–6560
17. M. Moglianetti, J. R. P. Webster, S. Edmondson, S. P. Armes and S. Titmuss, Langmuir, 2010, 26, 12684–12689
18. S. Sanjuan, P. Perrin, N. Pantoustier and Y. Tran, Langmuir, 2007, 23, 5769–5778
19. X. Bories-Azeau, S. P. Armes and H. J. W. van den Haak, Macromolecules, 2004, 37, 2348
20. V. Büttin, S. P. Armes and N. C. Billingham, Polymer, 2001, 42, 5993
21. X. Chen, D. P. Randall, C. Perruchot, J. F. Watts, T. E. Patten, T. von Werne and S. P. Armes, J. Colloid Interface Sci., 2003, 257, 56
22. S. Edmondson, C.-D. Vo, S. P. Armes and G.-F. Unali, Macromolecules, 2007, 40, 5271–5278
23. M. Geoghegan, L. Ruiz-Perez, C. C. Dang, A. J. Parnell, S. J.

-
- Martin, J. R. Howse, R. A. L. Jones, R. Golestanian, P. D. Topham, C. J. Crook, A. J. Ryan, D. S. Sivia, J. R. P. Webster and A. Menelle, *Soft Matter*, 2006, 2, 1076–1080
24. W. Li, H. Kong, C. Gao and D. Yan, *Chinese Science Bulletin*, 2005, 50, 2276–2280
25. A. J. Ryan, C. J. Crook, J. R. Howse, P. Topham, R. A. L. Jones, M. Geoghegan, A. J. Parnell, L. Ruiz-Pérez, S. J. Martin, A. Cadby, A. Menelle, J. R. P. Webster, A. J. Gleeson and W. Bras, *Faraday Discuss.*, 2005, 128, 55
26. P. D. Topham, J. R. Howse, C. J. Crook, A. J. Parnell, M. Geoghegan, R. A. L. Jones and A. J. Ryan, *Polym. Int.*, 2006, 55, 808–815
27. E. Stratakis, A. Mateescu, M. Barberoglou, M. Vamvakaki, C. Fotakis and S. H. Anastasiadis, *Chem. Commun.*, 2010, 46, 4136–4138
28. M. Biesalski and J. Rühe, *Langmuir*, 2000, 16, 1943–1950
29. L. Sun, G. L. Baker and M. L. Bruening, *Macromolecules*, 2005, 38, 2307–2314
30. M. Kimura, M. Sugawara, S. Sato, T. Fukawa and T. Mihara, *Chem.–Asian J.*, 2010, 5, 869–876
31. X. Chen and S. P. Armes, *Adv. Mater.*, 2003, 15, 1558
32. X. Y. Chen, S. P. Armes, S. J. Greaves and J. F. Watts, *Langmuir*, 2004, 20, 587–595
33. A. F. Stalder, G. Kulik, D. Sage, L. Barbieri and P. Hoffman, *Colloids Surf., A*, 2006, 286, 92
34. J. Henrie, S. Kellis, S. Schultz and A. Hawkins, *Opt. Express*, 2004, 12, 1464–1469
35. S. Edmondson, C.-D. Vo, S. P. Armes, G.-F. Unali and M. P. Weir, *Langmuir*, 2008, 24, 7208–7215
36. C.-D. Vo, A. Schmid, S. P. Armes, K. Sakai and S. Biggs, *Langmuir*, 2007, 23, 408
37. S. Edmondson and S. P. Armes, *Polym. Int.*, 2009, 58, 307–316
38. S. McDonald and S. P. Rannard, *Macromolecules*, 2001, 34, 8600
39. M. R. Tomlinson and J. Genzer, *Macromolecules*, 2003, 36, 3449
40. J.-B. Kim, W. Huang, M. D. Miller, G. L. Baker and M. L. Bruening, *J. Polym. Sci., Part A: Polym. Chem.*, 2003, 41, 386
41. R. Dong, M. Lindau and C. K. Ober, *Langmuir*, 2009, 25, 4774–4779
42. D. Aulich, O. Hoy, I. Luzinov, M. Brücher, R. Hergenröder, E. Bittrich, K.-J. Eichhorn, P. Uhlmann, M. Stamm, N. Esser and K. Hinrichs, *Langmuir*, 2010, 26, 12926–12932
43. E. P. K. Currie, A. B. Sieval, M. Avena, H. Zuilhof, E. J. R. Sudhölter and M. A. Cohen Stuart, *Langmuir*, 1999, 15, 7116–7118
44. T. Wu, P. Gong, I. Szleifer, P. Vlcek, V. Subr and J. Genzer, *Macromolecules*, 2007, 40, 8756–8764
45. W. D. Kumler and J. J. Eiler, *J. Am. Chem. Soc.*, 1943, 65, 2355–2361
46. Y. Perelygin and D. Chistyakov, *Russ. J. Appl. Chem.*, 2006, 79, 2041–2042
47. R. D. Wesley, T. Cosgrove, L. Thompson, S. P. Armes, N. C. Billingham and F. L. Baines, *Langmuir*, 2000, 16, 4467–4469
48. S. W. An, P. N. Thirtle, R. K. Thomas, F. L. Baines, N. C. Billingham, S. P. Armes and J. Penfold, *Macromolecules*, 1999, 32, 2731–2738
49. E. B. Zhulina, T. M. Birshtein and O. V. Borisov, *Macromolecules*, 1995, 28, 1491–1499
50. H. Zhang and J. Rühe, *Macromolecules*, 2005, 38, 4855–4860
51. G. Rossi, P. A. Pincus and P. G. Degennes, *Europhys. Lett.*, 1995, 32, 391–396
52. N. L. Thomas and A. H. Windle, *Polymer*, 1982, 23, 529–542
53. S. E. Creager and J. Clarke, *Langmuir*, 1994, 10, 3675–3683
54. I. Luzinov, S. Minko and V. V. Tsukruk, *Prog. Polym. Sci.*, 2004, 29, 635–698
55. P. A. FitzGerald, J. I. Amalvy, S. P. Armes and E. J. Wanless, *Langmuir*, 2008, 24, 10228–10234
56. M. Ramstedt, N. Cheng, O. Azzaroni, D. Mossialos, H. J. Mathieu and W. T. S. Huck, *Langmuir*, 2007, 23, 3314–3321